

Chapter 2

Fabrication of Ultra-High Density Silicon Nanowire Arrays

2.1 Introduction

Nanofabrication patterning of molecules as well as metals and semiconductor structures has received increasing attention. A major challenge in the development of robust nanopatterning techniques involves the reduction of feature size and the increase in pattern density. High-density nanoscale circuits have the potential to be more efficient and faster than the conventional electronic circuits. In addition, new scientific possibilities arise when the patterning techniques begin to approach the scales and densities of macromolecules, likely offering a feasible organic-inorganic interface to biological systems. In particular, nanowire (NW) circuit fabrication has become a very active field of research. To date, NWs have been used to fabricate modular circuit elements such as field-effect transistors (FETs),¹⁻⁴ bipolar junction transistors,⁵ p-n diodes,^{5,6} logic gates,^{7,8} lasers and LEDs,^{9,10} molecular memory,¹¹ and nanoscale electro-mechanical resonators.^{12, 13} In addition to NWs, the electronic, thermal and optical properties of single-walled carbon nanotubes (SWNTs) have been extensively studied.^{14, 15} In this chapter, I concentrate the discussion on the development of a robust and versatile technique to fabricate high-density silicon nanowire arrays. Significant

advantages afforded by such method lead to a variety of applications which are also briefly addressed here.

Silicon is an attractive material for multiple electronic applications. The physical and mechanical properties of silicon have been extensively studied and are well characterized. In addition, fabrication protocols for etching, patterning and electrically addressing silicon devices are highly developed. Finally, silicon-based devices are easily integrated into a conventional CMOS technology, thus providing an opportunity for large-scale manufacturing and commercialization. These reasons have sparked an extensive research into the fabrication techniques of silicon NWs (SiNWs) and their incorporation into functional devices. One such technique, which, at this time, is the most widely used method of SiNW fabrication for electronic applications, is the nanoparticle-catalyzed vapor-liquid-solid (VLS) growth mechanism.¹⁶⁻¹⁸ Briefly, a gold nanocluster is heated in the presence of vapor-phase silicon (SiH_4 in H_2) to 362 °C, a temperature of Au-Si eutectic, resulting in the formation of Au-Si alloy in the form of a liquid droplet. The droplet supersaturates in Si under a continuous flow of vapor Si, resulting in a precipitation of solid silicon. SiNW continues to grow from the solid-liquid interface as long as the droplet is supersaturated. This process may be tuned to produce single-crystal SiNWs with well-controlled diameter and growth orientation.¹⁹ However, this process also has major drawbacks, which limit its usefulness as a large-scale fabrication tool. One significant problem is the lack of precise control over the doping level. The VLS doping is done *in situ* by adding dopant precursor to the reaction, yielding NWs with doping levels and electrical properties which are largely unknown prior to their integration into a device. Additionally, while the VLS technique allows the

fabrication of many NWs at once, subsequent methods are required to align NWs into parallel arrays or crossbar circuits.¹⁷ One such method which has been the most successful in aligning VLS grown NWs employs a Langmuir-Blodgett (LB) trough.²⁰ Aside from being impractical for scaling up and manufacturing, LB method produces NWs with large alignment fluctuations and poor end-to-end registry of individual NWs. Interconnection and integration of such SiNW arrays into CMOS compatible circuitry is difficult.

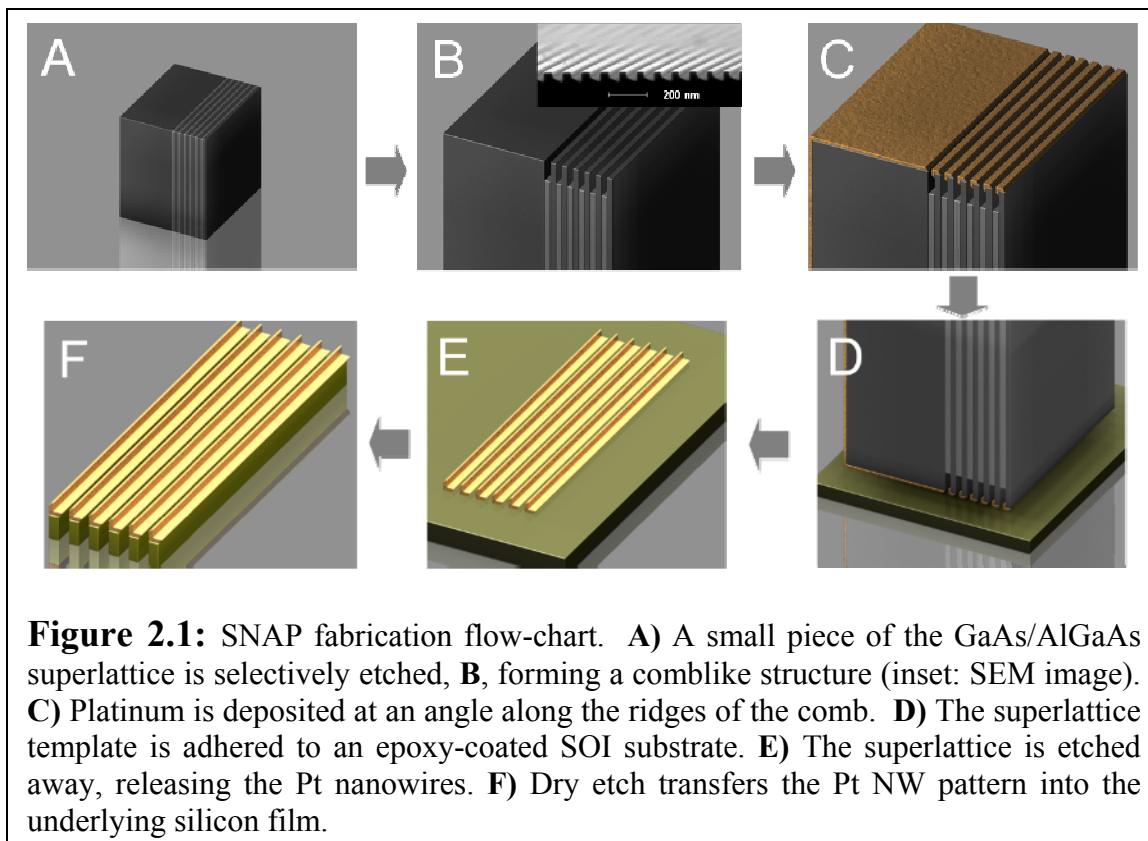
As described above, a major challenge in nanoelectronics is to be able to reproducibly fabricate high-density NW arrays with precise control over the diameter, length, pitch and doping level. Superlattice nanowire pattern transfer (SNAP) technique presented here, combined with the spin-on doping method (SOD), allows such level of control over multiple physical and electronic parameters of SiNWs, and may be extended to the fabrication of NWs from a wide range of materials. The other challenge is higher-order control of the device architecture, with arbitrary complex interconnections within an array of nanostructures. While certain ordered arrangements, such as nanowire crossbar structures,¹¹ are useful from the point of view of electronic circuit construction, many other applications require at least some level of nonperiodic complexity. Examples include routing networks between nanowire field-effect transistors,^{4, 21} or specified defects within photonic crystals. An extension of SNAP technique may be used to construct arbitrarily complex, two-dimensional nanowire structures templated on a single crystal substrate at sublithographic dimensions. As a proof-of-principle demonstration, this method is used to construct routing networks for Si nanowire-based complementary

symmetry logic applications with electrical contacts which are superior to those fabricated with other methods.

2.2 Superlattice Nanowire Pattern Transfer (SNAP)

Superlattice nanowire pattern transfer (SNAP)¹³ is a technique for fabricating aligned nanowires of a wide range of materials through a one-step deposition process without subsequent etching or liftoff, which is often necessary for other methods such as e-beam lithography (EBL).²² These fully formed NWs may be transferred to any surface. Further processing steps can be utilized to convert these nanowires into an identical pattern out of a thin-film material, such as silicon on insulator (SOI). SNAP technique has been developed to simultaneously address issues of NW size, pitch and alignment. NWs can be fabricated from a thin film of arbitrary material, as long as dry etching of such material is possible. Therefore, the electronic properties of the NWs produced via SNAP may be manipulated by a corresponding control of the properties of the starting thin film. For example, by combining SNAP technique with spin-on doping (SOD) method, a quantitative control of the NW doping level is possible.

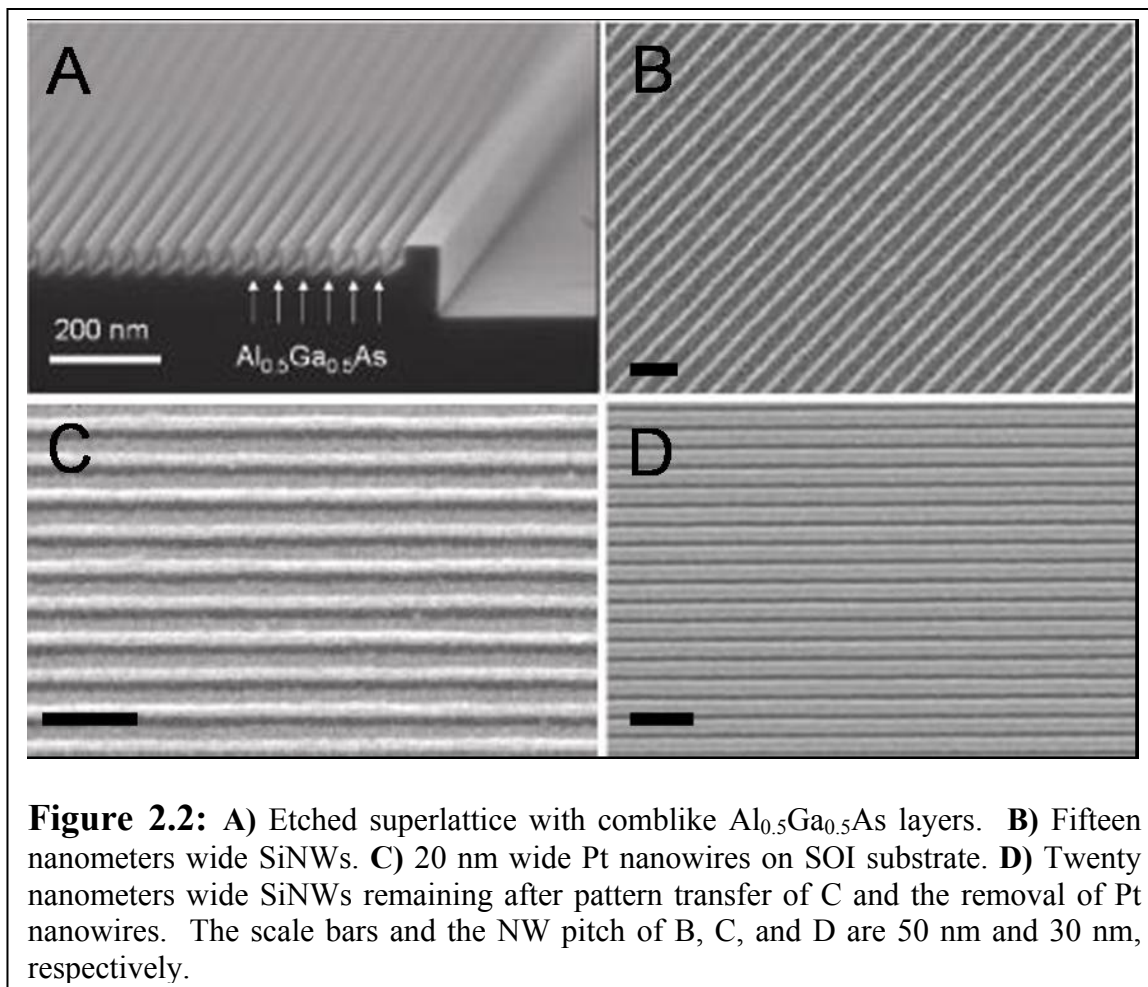
Figure 2.1 outlines the SNAP fabrication steps. SNAP uses molecular beam epitaxy (MBE) to create a physical template for NW patterning. Such template is a GaAs/Al_xGa_(1-x)As superlattice structure consisting of the alternating gallium-arsenide and aluminum-gallium-arsenide layers grown on top of a (100) GaAs substrate. The Al mole fraction may be varied between 0.5 and 0.8. The atomic-level control over the thickness and composition of each layer translates into atomic-level control over the resulting metal or semiconductor nanowires. The fabrication protocol begins by dicing a



portion of the superlattice wafer into 2 mm by 5 mm pieces, or masters (Figure 2.1A). Each master has one side, $\{110\}$ or $\{001\}$ plane, which is atomically flat. With that side facing up, the masters are placed into a Teflon holder and sonicated in methanol for ~ 10 seconds. The flat edge is swabbed until all microscopic particles are removed.

The GaAs layers are selectively etched in a solution of $\text{NH}_4\text{OH}/\text{H}_2\text{O}_2/\text{H}_2\text{O}$, producing a comblike structure shown in Figures 2.1B and 2.2A. The thickness of the AlGaAs layer determines the NW width, while the GaAs thickness translates into the distance between the NWs. A metal, such as platinum, is then deposited at an angle along the ridges of the AlGaAs layers on the atomically flat edge of the master (Figure 2.1C). The angle is chosen so that no metal is deposited on the etched GaAs layers, and is, therefore, dictated by the pitch of the NWs and the depth of the grooves in the superlattice comb structure. In general, NW pitches between 30 nm and 60 nm will

require a deposition angle between 45° and 15° with respect to the horizontal axis. The thickness of the deposited metal depends on the desired width of the NWs, and is generally 10 nm if the NW width is larger than 10 nm and equals to the NW width otherwise.



The metal-coated edge of the master is gently positioned on top of the epoxy-coated SOI surface which has been rigorously cleaned after the doping process described below (Figure 2.1D). The epoxy is heat curable, and consists of the mixture of Epoxy Bond 110 (Allied High Tech Products, Ranch Dominguez, CA, 10 drops part A to 1 drop part B) and 0.15 g of 6% PMMA in 20 mL of chlorobenzene. The epoxy is spun on the surface at 7000 RPM to form a film of approximately 10 nm thickness. Because the

master can be aligned on the surface at an arbitrary angle, SiNWs with crystal orientations between (100) and (110) along the length may be produced. The master-SOI substrate assembly is placed on the hot plate at 135 °C for 45 minutes, after which it is left in the solution of 1:5:50 (v/v/v) 30% H₂O₂:H₃PO₄:H₂O for ~5 hours, until all AlGaAs layers are etched, releasing the Pt NWs. The remaining master is detached from the substrate and the epoxy is removed in O₂ plasma. The remaining Pt nanowires (Figure 2.2C) are L shaped due to angular deposition onto the etched superlattice.

Reactive ion etching (RIE) may be used to transfer the pattern defined by the resulting Pt nanowires into an identical pattern in the silicon epilayer of SOI substrate. This is done with anisotropic etch in CF₄/He plasma (20/30 sccm, 5 mTorr, 40 W), which etches silicon at a rate of ~10 nm/min. Subsequently, Pt nanowires are removed in hot aqua regia (3:1 v/v HCl:HNO₃ at 120 °C for 20 minutes). As Figure 2.2 (B,D) demonstrates, the resulting SiNWs are straight, perfectly parallel, isolated from each other and have relatively smooth side walls. Since these wires are etched from the epilayer of the SOI substrate, they are also electrically isolated from one another. The procedure to convert the Si nanowires into functioning devices for biological sensing and thermoelectric applications is described in details in the following chapters. It is critical to emphasize the versatility afforded by the SNAP technique. First, various metal NWs may be fabricated on any substrate; so far, the metals which have successfully yielded NWs are gold, chromium, aluminum, titanium, niobium, platinum and nickel.¹³ Second, NWs from any thin film material may be fabricated, provided that anisotropic etch for that material exists. Third, physical parameters such as the number of parallel NWs, their

sizes, pitches and lengths are precisely controlled. Finally, the electronic properties of SiNWs can be tightly modulated with quantitative doping of the initial thin silicon film.

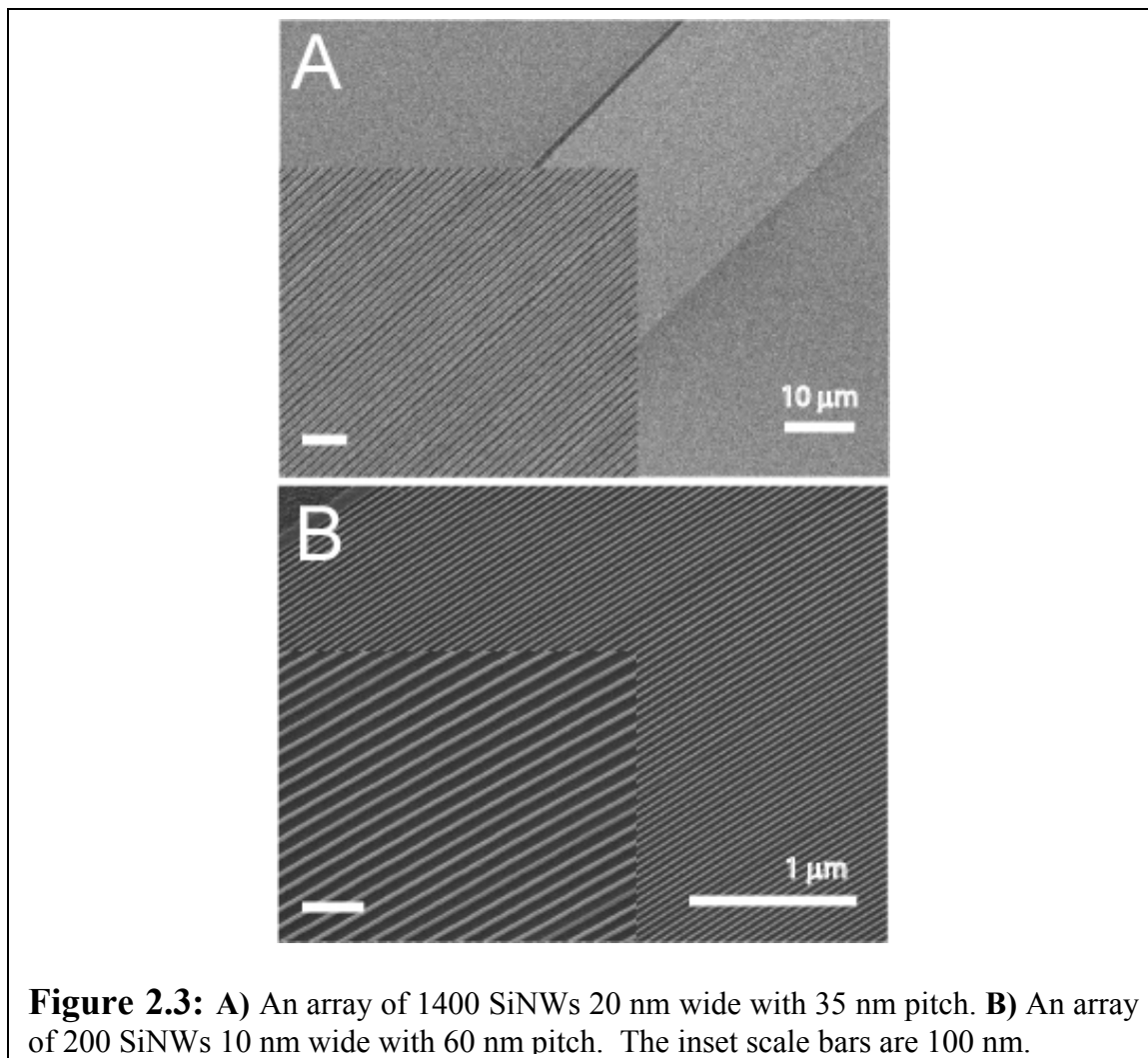


Figure 2.3: **A)** An array of 1400 SiNWs 20 nm wide with 35 nm pitch. **B)** An array of 200 SiNWs 10 nm wide with 60 nm pitch. The inset scale bars are 100 nm.

The size of the array containing SiNWs is only limited by the MBE growth time, and could, in principle, be increased to thousands of NWs. Figure 2.3A demonstrates the largest array produced so far with SNAP technique, containing 1400 SiNWs with 20 nm width. The diameter of the NWs may also, in principle, be significantly decreased to about 1 nm or less, owing to atomic-level control of the MBE process. In practice, however, it has been rather difficult to reproducibly obtain SiNWs thinner than ~7 nm, although it certainly is not by any means the limit of the technique. Ten-nanometers-

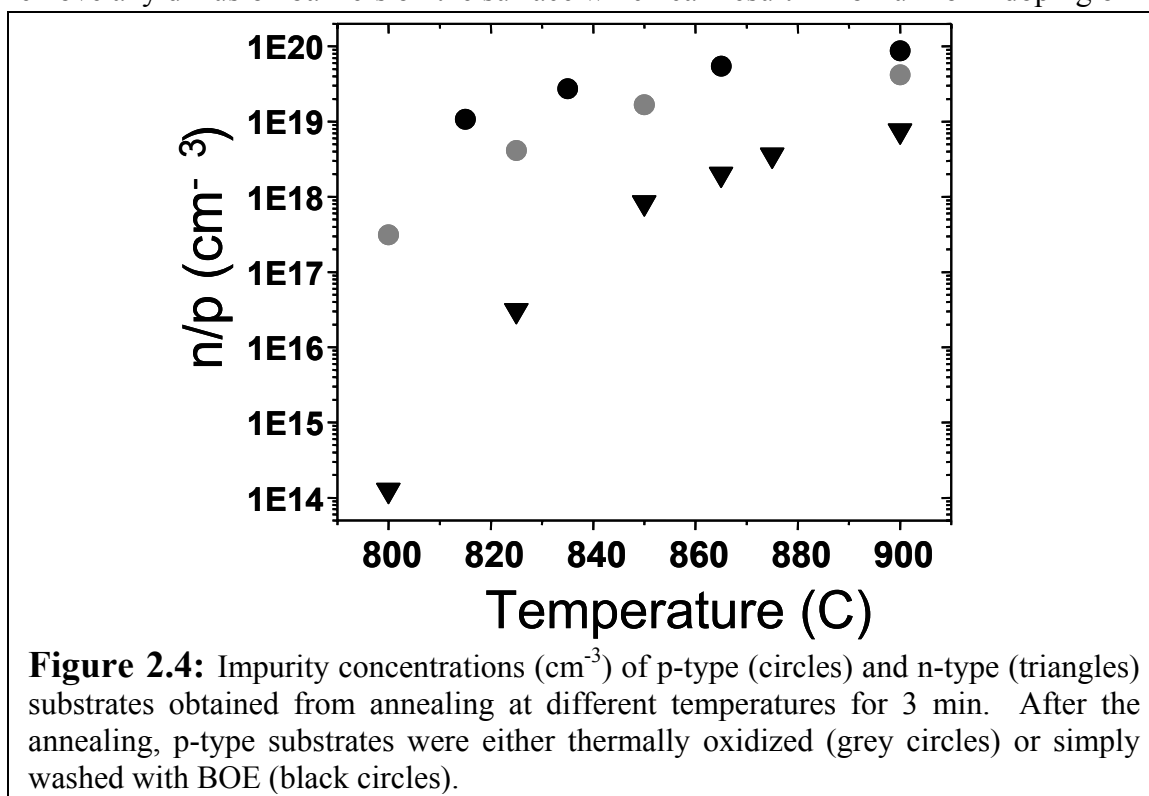
wide NWs (Figure 2.3B) have been extensively studied in context of, for example, silicon thermoelectric properties (chapter five).

2.3 Diffusion Doping of Silicon Thin Films

As mentioned above, a major advantage of SNAP technique is that the starting material is a thin film, the electrical properties of which are much easier to control through doping than those of NWs grown via VLS technique. A large SOI surface can be uniformly doped and used to produce multiple SiNW arrays, all of which will have an identical concentration of impurities. This allows us to carry out systematic studies of the effects of doping concentration on, for example, the electrical and thermoelectrical properties of NWs. These studies generally require many NW samples whose doping levels are quantified and are the same. For this purpose we have utilized spin-on doping (SOD) technique, which is based on the thermally mediated impurity diffusion. SOD method has several very important advantages over other thin-film doping techniques, such as ion implantation. Ion implantation, which uses high energy ion flux, results in the lattice damage of the SOI substrate and the reduction the electrical conductivity of the NWs.²³ The diffusion doping process, on the other hand, does not lead to the damage of thin silicon film. The other practical advantage of SOD technique is that the doping may be tuned over a large range of concentrations by simply varying the temperature. This may be readily done on small wafer pieces, introducing the flexibility which is lacking when large wafers have to be sent out for ion implantation. In addition, patterned diffusion doping of the thin-film substrate is necessary to create more complicated

circuits such as complementary logic gates, where n-type and p-type FETs must exist on the same device in close proximity.⁸

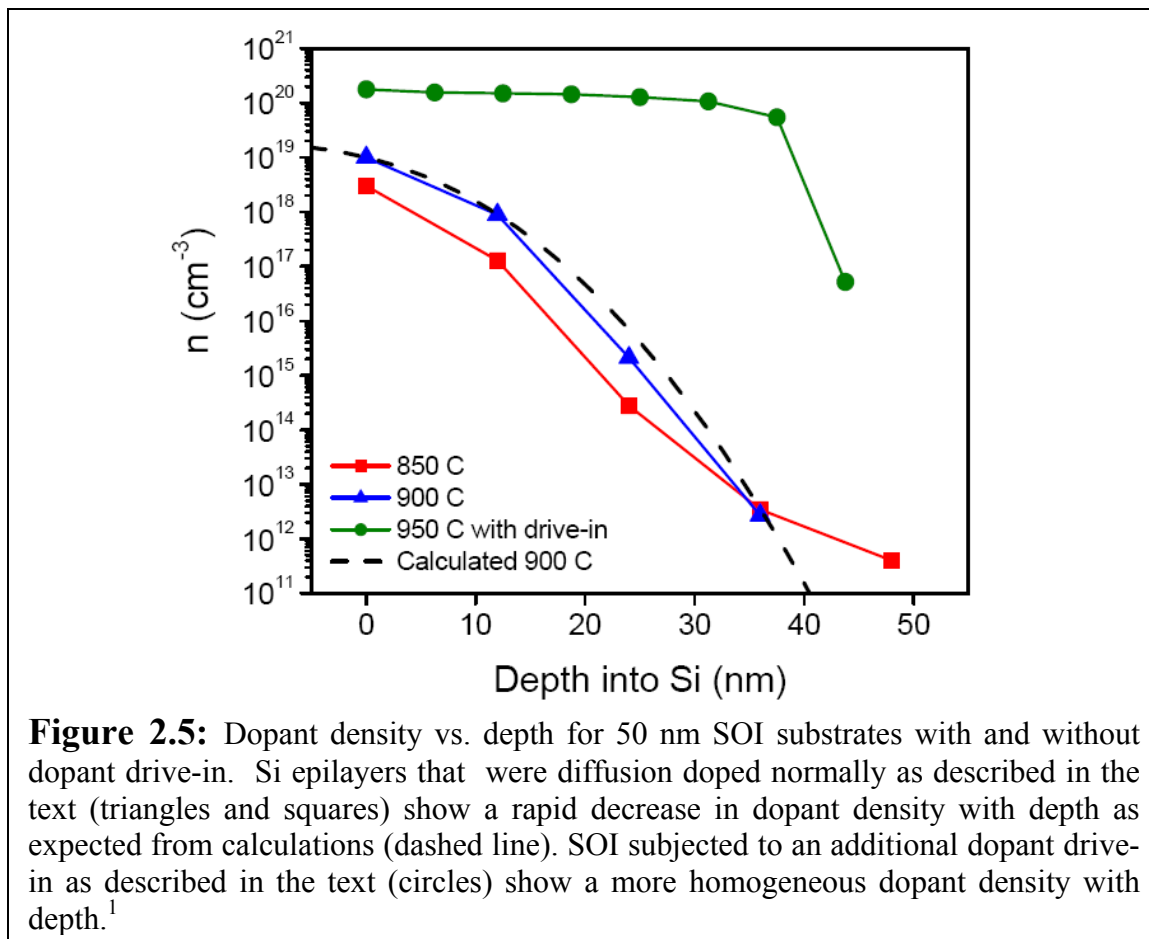
The SOD procedure consists of four steps: wafer cleaning, application of the dopant, annealing and removal of the dopant. Wafers have to be thoroughly cleaned to remove any diffusion barriers on the surface which can result in non-uniform doping of



the substrate. RCA clean is used: 5:1:1 $\text{H}_2\text{O}/\text{H}_2\text{O}_2/\text{NH}_4\text{OH}$ for 10 min at 80°C , followed by the removal of oxide in dilute (50:1 $\text{H}_2\text{O}/\text{HF}$) hydrofluoric acid, followed by 6:1:1 $\text{H}_2\text{O}/\text{H}_2\text{O}_2/\text{HCl}$ for 10 min at 80°C . The wafers are rinsed with H_2O and a thin film of dopants is spun on the surface. Most spin-on dopants consist of the desired species (such as phosphorus or boron) incorporated into a silica or organic polymer matrix dissolved in an organic solvent. For all the applications in this thesis, Boron A organic film (Filmtronics, Bulter, PA) was used to produce p-type substrates, while phosphorosilica (Emulsitone, Whippany, NJ) films generated n-type devices. Thin films of dopant were

baked on a hot plate for 10 min at 200 °C prior to the annealing. Rapid thermal annealer (RTA) was used to precisely control the temperature and time of the annealing, which was carried out under nitrogen. Usually, the temperature was varied and the time was maintained at 3 min to achieve different doping concentrations. Figure 2.4 summarizes the annealing conditions and the impurity concentrations they yield. After the annealing, phosphorosilica film was removed simply by immersion in BOE for a few seconds, resulting in a hydrophobic surface. Boron A film, however, could not usually be completely removed with BOE, as indicated by the hydrophilicity of the substrate. For applications such as biological sensing, where a hydrophobic surface is required at this step to assure the presence of exposed oxide later for subsequent surface functionalization, the substrates were thermally oxidized in RTP for a minute in pure oxygen at the same temperature as the previous annealing step. After the oxidation and BOE treatment, hydrophobic surface could be reliably obtained. The thermal oxidation, however, somewhat lowered the impurity doping (Figure 2.4), probably because of the oxidation and removal of the top few layers of the silicon.

The electrical resistivity of the thin film was measured with 4-point technique²⁴ by applying a 10 mA DC current between the outer pins and measuring the voltage drop across the inner pins. The resistivity was converted to the approximate impurity concentration by using the reference tables generated for bulk silicon.²⁴ The doping profile as a function of depth into the silicon epilayer was determined experimentally (Figure 2.5, blue triangles and red squares) by thinning a 50 nm Si epilayer in 10 nm steps via CF₄ etching, each time measuring the electrical resistivity of the film. Diffusion

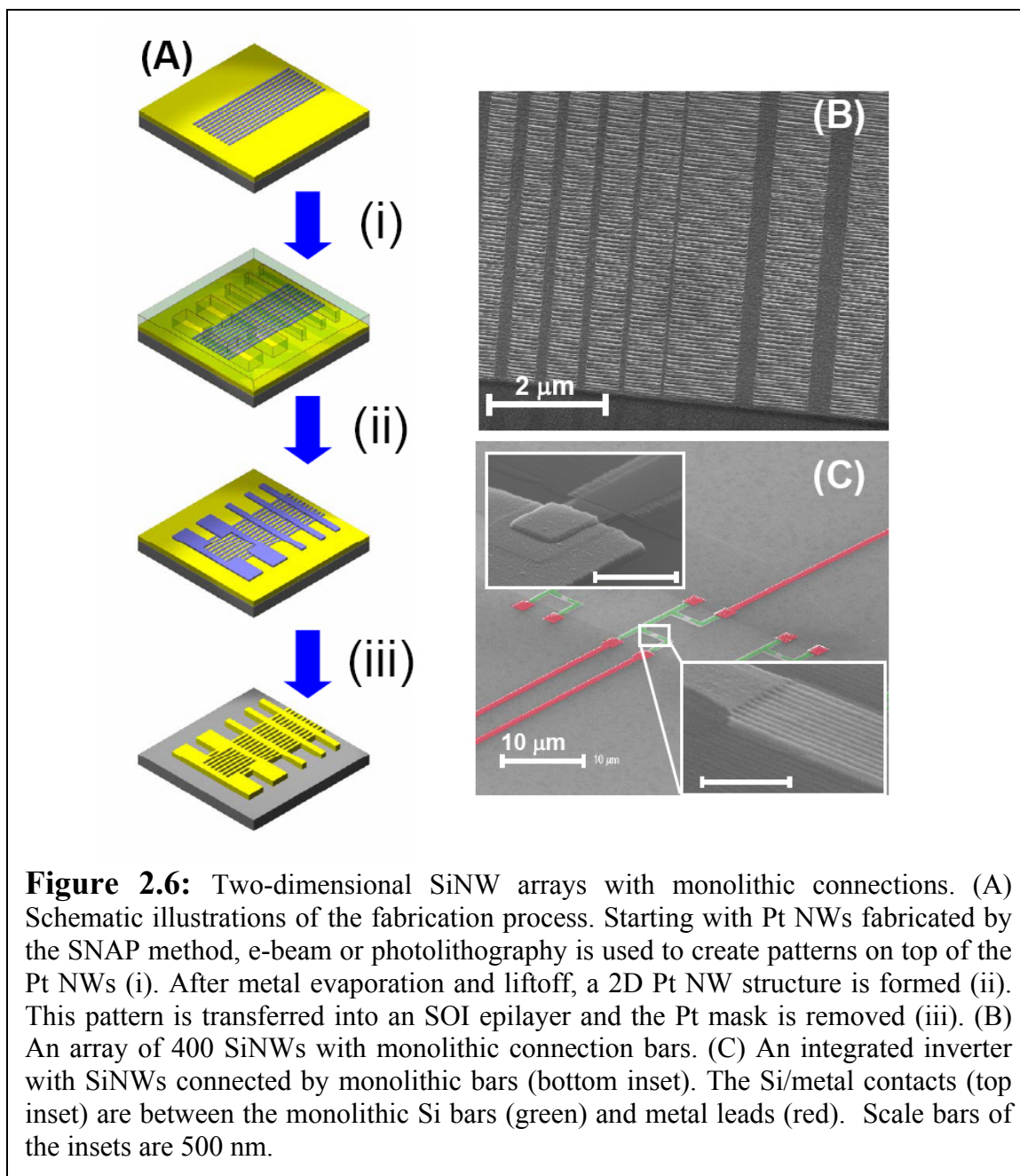


doping produces an impurity gradient which falls rapidly away from the surface. The model of the infinitely thick Si epilayer (Figure 2.5, dashed line) agrees well with the experimental data.¹ The inhomogeneous doping profile shown in Figure 2.5 has important implications for a variety of applications, as will be described later in this chapter. However, there are cases when a homogeneous doping is required. An additional annealing step is then used. The dopant film is removed as described above and ~250 nm of SiO₂ is deposited (PECVD) on the substrate. Subsequently, the wafer is annealed at 1000 °C for 10-15 minutes to produce a homogeneous doping profile shown in Figure 2.5 (green circles).¹

2.4 Two-Dimensional Nanowire Circuits

As described above, high-density nanocircuits with more complex architectures such as a crossbar are usually fabricated either using EBL or, in the case of VSI SiNWs²⁰ or SWNTs^{25, 26}, utilizing Langmuir-Blodgett trough technique or an AC electric field, respectively. All these methods are serial and generally produce functional devices with low yield, making them sufficient only for one-off demonstrations. Being a top-down approach, SNAP may be easily extended to fabricate more complicated two-dimensional (2D) circuits for a variety of applications. For example, the production of 2D SiNW logic and routing circuits at sublithographic dimensions involves combining SNAP process with other patterning techniques such as e-beam lithography (EBL). The unprecedented dimension and density that can be achieved by the SNAP method for the production of aligned NW arrays is complemented by the arbitrary complexity that can be achieved via the incorporation of traditional patterning methods.

In a typical process, as demonstrated in Figure 2.6A, an array of Pt NWs is first deposited by the SNAP technique onto an SOI substrate as described above. The substrate is then further patterned using electron beam lithography to generate arbitrarily complex structures on top of the first set of Pt NWs. After the evaporation and subsequent liftoff of 20 Å Ti (as a sticking layer) and 100 Å Pt, a 2D structure consisting of Pt NWs and perpendicular Pt bars is obtained. Pt is then used as an etch mask to transfer the pattern into the underlying SOI epilayer via a directional dry etching with CF₄ gas. The entire process is concluded with the removal of Pt NWs and bars in aqua regia (Figure 2.6A). The resulting 2D Si structure consists of NWs connected by arbitrary routing bars, all formed from a single-crystalline layer of Si. Figure 2.6B shows an array



of 400 20 nm wide SiNWs with a pitch of 33 nm. The NWs are connected by Si bars with various widths, ranging from 50 to 500 nm. Alternatively, instead of connecting them all at once, a subset of NWs can be selectively connected, as shown in Figure 2.6C. This structure can be used to fabricate, among other things, integrated electronic logic gates. The false color-coded green structures in Figure 2.6C are current routing bars,

which are single crystalline extensions of the SiNWs. They negate the need for direct electrical contacts to the nanowires. The device depicted in Fig 2.6C is a complementary symmetry inverter, or NOT gate.

The monolithic NW structure can be utilized to form high-quality and reliable electrical contacts which are crucial for any application such as high performance NW field effect transistors (FETs), thermoelectrics (chapter 5) or SiNW biosensors (Chapter 3). Despite enormous efforts by various researchers, obtaining reliable electrical contacts to SiNWs ~10-20 nm wide using metal pads remains a challenge. Because of the high surface-to-volume ratio, NWs are more sensitive to surface states than their bulk counterparts.^{8,27} Electrical contacts to the NWs, therefore, are significantly influenced by the surface states and their quality depends on particular steps in the fabrication process, such as contact annealing. Often, these necessary processing steps vary significantly for n-type and p-type Si FETs. Single-crystalline, 2D SiNW circuits may represent a universal solution to this challenging problem. First, the electrical contacts to the NWs are established through relatively large Si pads, rather than through the NWs themselves (Figure 2.6C). These types of metal/Si contacts are less sensitive to the surface states and have been extensively studied and optimized for conventional MOSFET fabrication. Second, the doping levels within contact regions and those of NWs may be separately optimized, as described later in the text. Finally, the routing Si bars can have an arbitrarily complex architecture (Figure 2.6C).

As described in the previous section, diffusion doping of SOI epilayer results in an impurity gradient, with highest doping concentration at the silicon surface (Figure 2.5). Depending on the doping conditions, the impurity density can decrease by a factor of 10

to 100 at a distance of ~ 10 nm below the top NW surface. Such sharp gradient can assist in separately modulating the NW and contact doping levels. High impurity concentration, in general, means that the Fermi level of the NWs is close to or in the conduction (n-type) or the valence band (p-type). As a result, the changes in the gate potential are inadequate to significantly alter the Fermi level, and the channel resistance of an FET does not change appreciably, yielding a poor gate modulation. Heavily doping NWs, on the other hand, results in a short depletion width within Si and a narrow Schottky barrier between metal and Si. Charge transfer through the contact region is, therefore, highly efficient. Such contact is less sensitive to the surface states due to the reduced depletion width. Overall, a heavily doped semiconductor forms good electrical contact but does not respond well to gate modulation. Conversely, the Fermi level of a lightly doped semiconductor is typically in the midgap, slightly deviating toward the conduction (n-type) or valence band (p-type). Small changes in the gate potential cause large shifts of the Fermi level and an efficient gate modulation. However, a lower doping level also means a longer depletion width, making the FET body very sensitive to surface and interface states. In general, it is difficult to establish good electrical contacts to lightly doped silicon.

An ideal FET structure exhibits different doping profiles in different regions: the source-drain (S-D) channel is lightly doped, while the S and D contact regions are heavily doped. Conventional FET structures are fabricated with such inhomogeneous doping profiles, which are achieved using ion implantation methods. To avoid damaging the NWs, alternative approaches are required to achieve similar doping profiles.²³ In meeting this challenge, various approaches have been reported. These include the

formation of metal silicides at the NW S and D contacts²⁸ or synthesizing NWs with axially heterogeneous doping profiles.^{29,30} While promising initial results exist, reliability in forming high quality contacts has not been demonstrated yet. Our approach to create inhomogeneous doping profiles along the FET channel involves a two-step process. FETs are first fabricated with the entire body, including the channel and semiconductor/metal interface, doped heavily (i.e. $>10^{19}$ cm⁻³). After the deposition of metal contacts, anisotropic etching with CF₄ gas removes the top (heavily doped) layers of Si. Metal contacts protect the S/D silicon regions, which remain heavily doped.

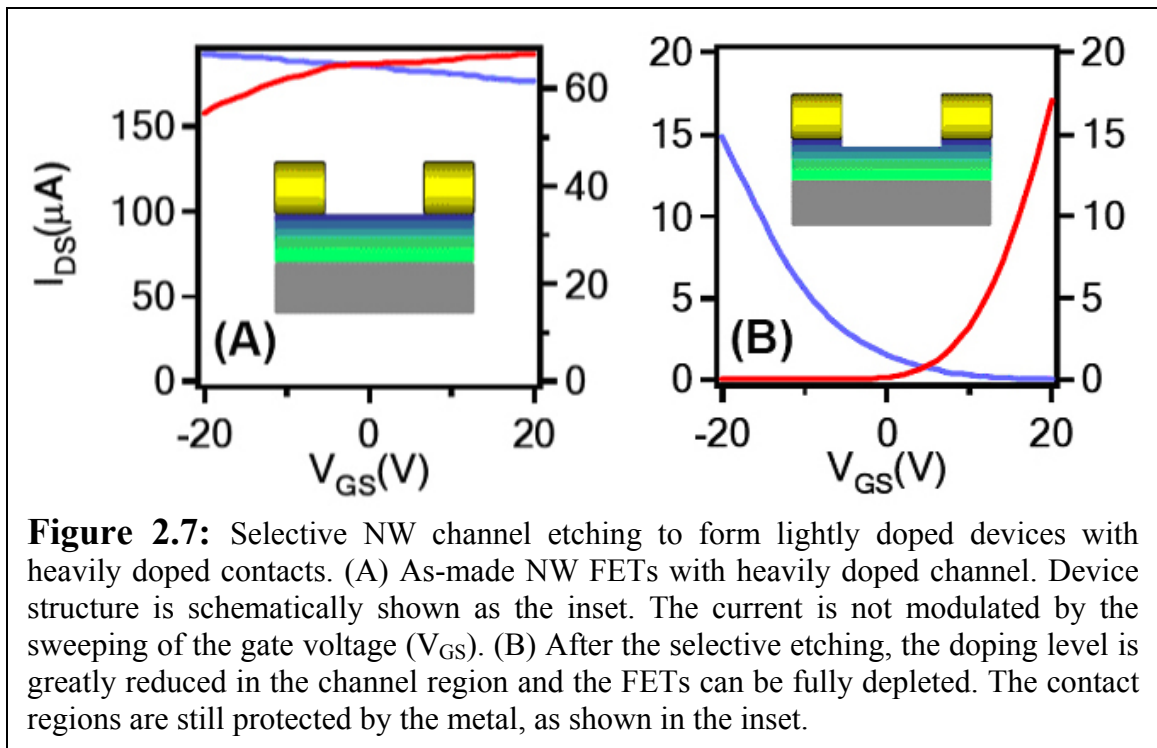
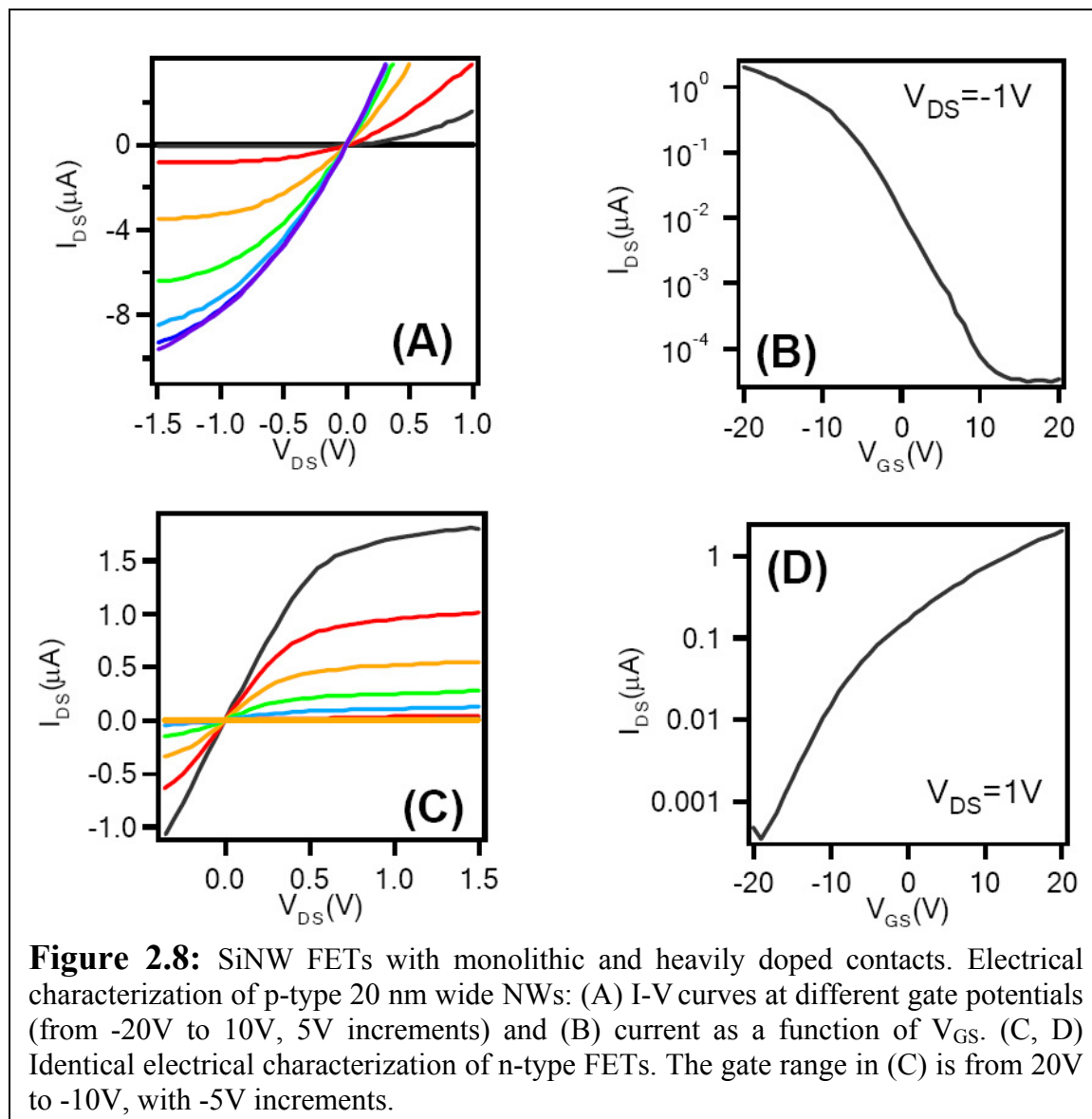


Figure 2.7: Selective NW channel etching to form lightly doped devices with heavily doped contacts. (A) As-made NW FETs with heavily doped channel. Device structure is schematically shown as the inset. The current is not modulated by the sweeping of the gate voltage (V_{GS}). (B) After the selective etching, the doping level is greatly reduced in the channel region and the FETs can be fully depleted. The contact regions are still protected by the metal, as shown in the inset.

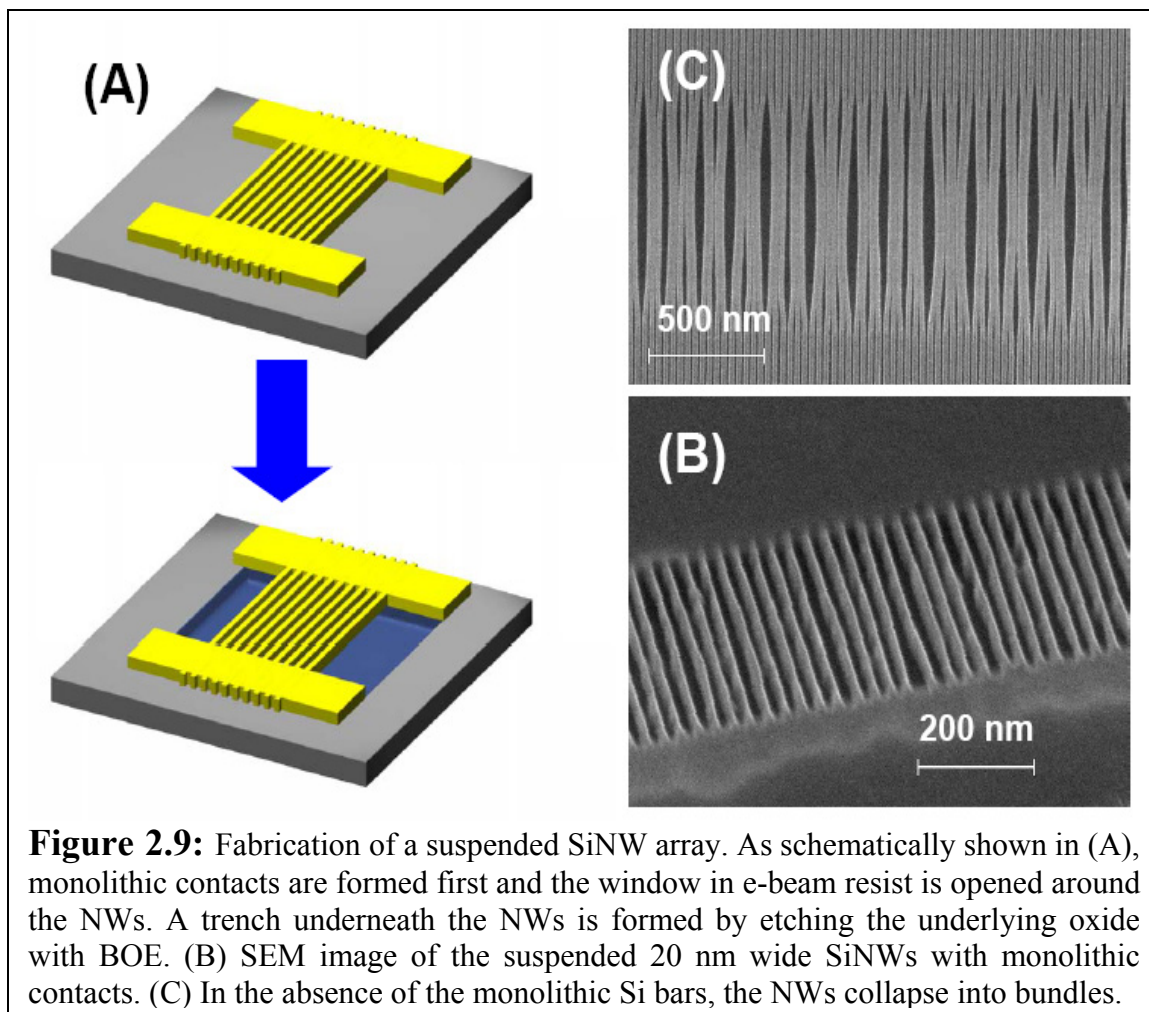
The effect of selective CF₄ etching described above is clearly demonstrated in Figure 2.7. Initially, the devices are highly doped and the source/drain (S/D) conductance changes little when the bottom gate is swept from -20 to 20 V (Figure 2.7A). After the etching, the reduced channel doping level yields a much better gate modulation: the S/D conductance changes by more than 3 orders of magnitude in the same range of

the gate voltage (Figure 2.7B). Importantly, this method is compatible with both p- and n-type FETs. The development of a single process which can be applied to both p- and n-type NW FETs is enabling for power-efficient complementary symmetry NW logic applications.⁸ Alternatively, one must rely on different annealing methods or other phenomenological treatments to get reliable contacts to NW FETs.²⁸

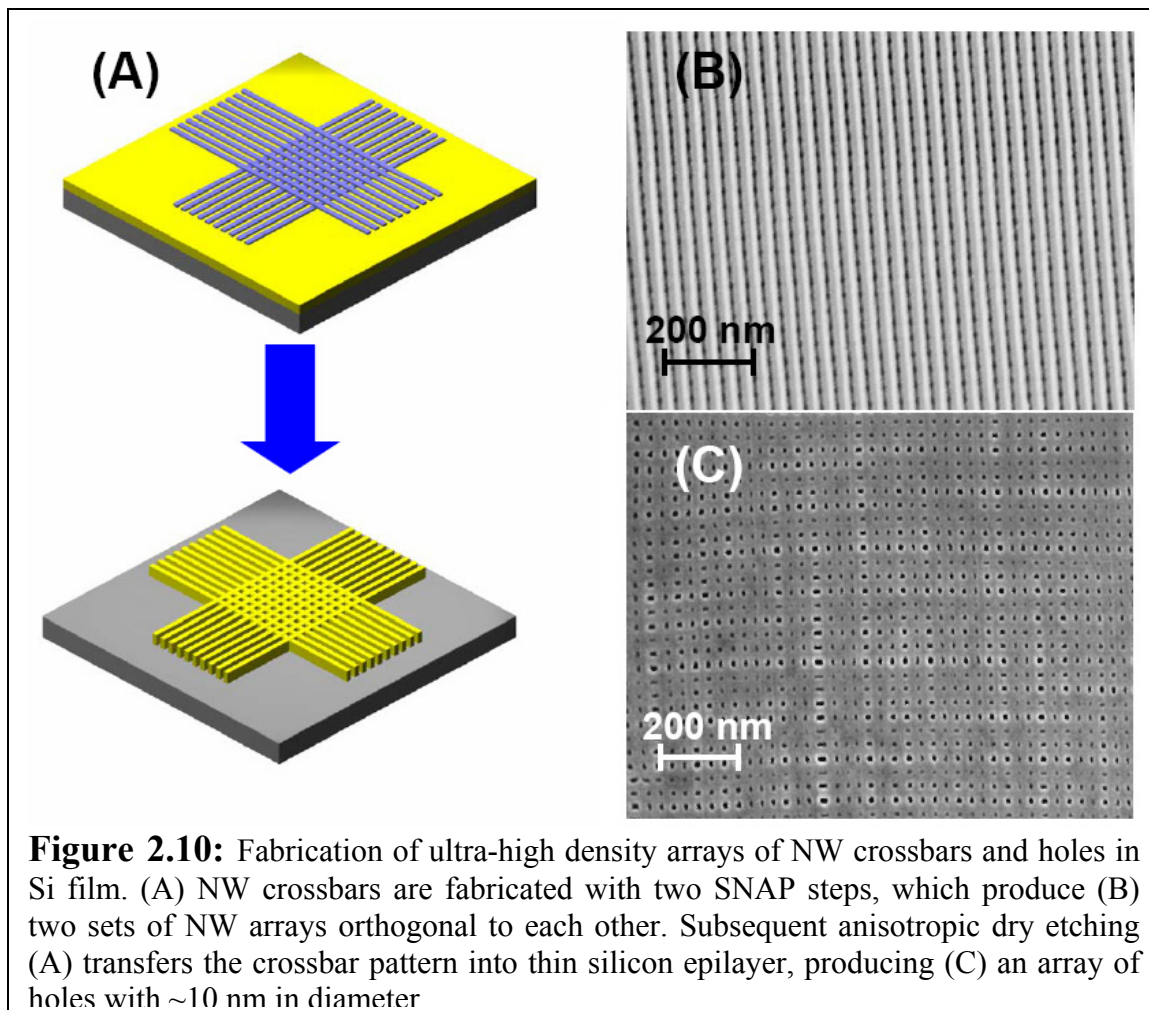


Combining the selective channel etching and the monolithic structures yields high quality electrical contacts (Figure 2.8). For both p- and n-FETs, the linear I-V behavior

in the low-bias regions at all measured gate potentials indicates that the contacts are ohmic. Corresponding current versus gate voltage traces reveal that the FET conductance can be modulated with high efficacy. Furthermore, this method is highly reliable and reproducible. For more than 100 devices, less than twenty percent variation in the on-current was observed from device to device.



In addition to constructing reliable, NW-based complementary symmetry logic circuits, the 2D patterning methods can be extended towards the production of a host of other novel and potentially useful structures as well. A first example is shown in Figure 2.9. Ultra-dense arrays of SiNWs can be suspended, thus allowing for the measurements of thermal properties of nanowires³¹ or for creating high-frequency NW resonators.¹²



When an array of aligned, closely spaced NWs is suspended over a trench, various processing steps, coupled with the van der Waals interactions between the NWs, inevitably cause NWs to collapse into bundles (Figure 2.9B). The integrity of the suspended NWs can be maintained by fixing them on either end with an in-plane monolithic structure of the type described above (Figure 2.9C). Nevertheless, it is worth pointing out that this method does have its limitations. When the trench is too wide, proximity of the NWs still may cause them to collapse together, even in the presence of the monolithic bars.

Multiple SNAP transfers can also be utilized in sequence to generate different three-dimensional circuits. For example, two orthogonal NW arrays may be constructed for applications in ultra-high density molecular memory based on the crossbar architecture (Figure 2.10B).¹¹ Crossbar devices of this type may be further used to fabricate arrays of nanometer diameter holes in silicon with nanometer spacing (Figure 2.10). The nanohole arrays can be tuned in a number of ways. First, their diameter can be adjusted by using NW superlattice with a different pitch. Second, the spacing between holes can be tuned by using NWs of different widths. Third, their shape can be changed by aligning the two sets of NW arrays at different angles. The nanohole arrays are of some interest and potentially useful in photonic applications.³²⁻³⁴

2.5 Discussion

As demonstrated in this chapter, Superlattice Nanowire Pattern Transfer (SNAP) is a very versatile technique for the fabrication of high-density nanowires from a wide range of materials, including silicon. Important advantages of SNAP over other SiNW fabrication methods, such as VLS technique, allow for systematic studies of the fundamental properties of nanowires which go beyond one-off device demonstrations. SNAP allows precise control over the number, width, spacing and length of the nanowires. In addition, perfectly parallel arrays of NWs are fabricated, eliminating the necessity for complicated alignment techniques such as those utilizing Langmuir-Blodgett trough. Complicated circuits, therefore, may be readily fabricated with high precision and yield. In addition, the top-down nature of SNAP means that the impurity levels of NWs can be carefully controlled by standard thin-film diffusion doping methods. As demonstrated here and in the following chapters, it is critical to be able to

systematically and quantitatively manipulate the dopant concentrations for optimizing the electrical properties of SiNW-based FETs, thermoelectrics and biological sensors. Using the traditional lithography in combination with SNAP yields 2D NW circuitry of arbitrary complexity. Reproducibly obtaining high quality contacts to SiNWs is a major challenge. However, by integrating an additional processing step, very high quality metal/Si contacts to 10 nm wide SNAP NWs can be fabricated. Robustness and versatility of the technique, ease of fabrication and the quality of the produced nanomaterial are central issues in nanoelectronics. SNAP exhibits superior performance in each of these categories.

Bibliography

1. Beckman, R.; Johnston-Halperin, E.; Luo, Y.; Green, J. E.; Heath, J. R., Bridging dimensions: Demultiplexing ultrahigh-density nanowire circuits. *Science* **2005**, 310, (5747), 465-468.
2. Duan, X. F.; Huang, Y.; Cui, Y.; Wang, J. F.; Lieber, C. M., Indium phosphide nanowires as building blocks for nanoscale electronic and optoelectronic devices. *Nature* **2001**, 409, (6816), 66-69.
3. Cui, Y.; Zhong, Z. H.; Wang, D. L.; Wang, W. U.; Lieber, C. M., High performance silicon nanowire field effect transistors. *Nano Lett.* **2003**, 3, (2), 149-152.
4. Wang, D. W.; Sheriff, B. A.; Heath, J. R., Silicon p-FETs from ultrahigh density nanowire arrays. *Nano Lett.* **2006**, 6, (6), 1096-1100.
5. Cui, Y.; Lieber, C. M., Functional nanoscale electronic devices assembled using silicon nanowire building blocks. *Science* **2001**, 291, (5505), 851-853.
6. Huang, Y.; Duan, X. F.; Cui, Y.; Lieber, C. M., Gallium nitride nanowire nanodevices. *Nano Lett.* **2002**, 2, (2), 101-104.
7. Huang, Y.; Duan, X. F.; Cui, Y.; Lauhon, L. J.; Kim, K. H.; Lieber, C. M., Logic gates and computation from assembled nanowire building blocks. *Science* **2001**, 294, (5545), 1313-1317.
8. Wang, D. W.; Sheriff, B. A.; Heath, J. R., Complementary symmetry silicon nanowire logic: Power-efficient inverters with gain. *Small* **2006**, 2, (10), 1153-1158.
9. Pauzauskie, P. J.; Sirbuly, D. J.; Yang, P. D., Semiconductor nanowire ring resonator laser. *Phys. Rev. Lett.* **2006**, 96, (14).
10. Pauzauskie, P. J.; Yang, P., Nanowire photonics. *Mater. Today* **2006**, 9, (10), 36-45.
11. Green, J. E.; Choi, J. W.; Boukai, A.; Bunimovich, Y.; Johnston-Halperin, E.; DeIonno, E.; Luo, Y.; Sheriff, B. A.; Xu, K.; Shin, Y. S.; Tseng, H. R.; Stoddart, J. F.; Heath, J. R., A 160-kilobit molecular electronic memory patterned at 10(11) bits per square centimetre. *Nature* **2007**, 445, (7126), 414-417.
12. Husain, A.; Hone, J.; Postma, H. W. C.; Huang, X. M. H.; Drake, T.; Barbic, M.; Scherer, A.; Roukes, M. L., Nanowire-based very-high-frequency electromechanical resonator. *Appl. Phys. Lett.* **2003**, 83, (6), 1240-1242.
13. Melosh, N. A.; Boukai, A.; Diana, F.; Gerardot, B.; Badolato, A.; Petroff, P. M.; Heath, J. R., Ultrahigh-density nanowire lattices and circuits. *Science* **2003**, 300, (5616), 112-115.
14. McEuen, P. L.; Fuhrer, M. S.; Park, H. K., Single-walled carbon nanotube electronics. *IEEE Trans. Nanotechnol.* **2002**, 1, (1), 78-85.
15. Dai, H. J., Carbon nanotubes: Opportunities and challenges. *Surf. Sci.* **2002**, 500, (1-3), 218-241.
16. Morales, A. M.; Lieber, C. M., A laser ablation method for the synthesis of crystalline semiconductor nanowires. *Science* **1998**, 279, (5348), 208-211.
17. Lu, W.; Lieber, C. M., Semiconductor nanowires. *J. Phys. D* **2006**, 39, (21), R387-R406.

18. Yang, P. D., The chemistry and physics of semiconductor nanowires. *MRS Bulletin* **2005**, 30, (2), 85-91.
19. Wu, Y.; Cui, Y.; Huynh, L.; Barrelet, C. J.; Bell, D. C.; Lieber, C. M., Controlled growth and structures of molecular-scale silicon nanowires. *Nano Lett.* **2004**, 4, (3), 433-436.
20. Whang, D.; Jin, S.; Wu, Y.; Lieber, C. M., Large-scale hierarchical organization of nanowire arrays for integrated nanosystems. *Nano Lett.* **2003**, 3, (9), 1255-1259.
21. Zhong, Z. H.; Wang, D. L.; Cui, Y.; Bockrath, M. W.; Lieber, C. M., Nanowire crossbar arrays as address decoders for integrated nanosystems. *Science* **2003**, 302, (5649), 1377-1379.
22. Vieu, C.; Carcenac, F.; Pepin, A.; Chen, Y.; Mejias, M.; Lebib, A.; Manin-Ferlazzo, L.; Couraud, L.; Launois, H., Electron beam lithography: resolution limits and applications. *Appl. Surf. Sci.* **2000**, 164, 111-117.
23. Beckman, R. A.; Johnston-Halperin, E.; Melosh, N. A.; Luo, Y.; Green, J. E.; Heath, J. R., Fabrication of conducting Si nanowire arrays. *J. Appl. Phys.* **2004**, 96, (10), 5921-5923.
24. Sze, S. M., *Physics of Semiconductor Devices*, 2nd ed. Taipei: John Wiley & Sons, 1981.
25. Diehl, M. R.; Yaliraki, S. N.; Beckman, R. A.; Barahona, M.; Heath, J. R., Self-assembled, deterministic carbon nanotube wiring networks. *Angew. Chem., Int. Ed.* **2001**, 41, (2), 353.
26. Yan, Y. H.; Chan-Park, M. B.; Zhang, Q., Advances in carbon-nanotube assembly. *Small* **2007**, 3, (1), 24-42.
27. Wang, D. W.; Chang, Y. L.; Wang, Q.; Cao, J.; Farmer, D. B.; Gordon, R. G.; Dai, H. J., Surface chemistry and electrical properties of germanium nanowires. *J. Am. Chem. Soc.* **2004**, 126, (37), 11602-11611.
28. Weber, W. M.; Geelhaar, L.; Graham, A. P.; Unger, E.; Duesberg, G. S.; Liebau, M.; Pamler, W.; Cheze, C.; Riechert, H.; Lugli, P.; Kreupl, F., Silicon-nanowire transistors with intruded nickel-silicide contacts. *Nano Lett.* **2006**, 6, (12), 2660-2666.
29. Yang, C.; Barrelet, C. J.; Capasso, F.; Lieber, C. M., Single p-type/intrinsic/n-type silicon nanowires as nanoscale avalanche photodetectors. *Nano Lett.* **2006**, 6, (12), 2929-2934.
30. Yang, C.; Zhong, Z. H.; Lieber, C. M., Encoding electronic properties by synthesis of axial modulation-doped silicon nanowires. *Science* **2005**, 310, (5752), 1304-1307.
31. Li, D.; Wu, Y.; Kim, P.; Shi, L.; Yang, P.; Majumdar, A., Thermal conductivity of individual silicon nanowires. *Appl. Phys. Lett.* **2003**, 83, (14), 2934-2936.
32. Joannopoulos, J. D.; Villeneuve, P. R.; Fan, S. H., Photonic crystals: Putting a new twist on light. *Nature* **1997**, 386, (6621), 143-149.
33. Qiu, M.; He, S. L., Large complete band gap in two-dimensional photonic crystals with elliptic air holes. *Phys. Rev. B* **1999**, 60, (15), 10610-10612.
34. Yablonovitch, E., Photonic band-gap structures. *J. Optic. Soc. Am. B* **1993**, 10, (2), 283-295.